Desalination and Water Treatment
www.deswater.com
doi:10.5004/dwt.2016.0154

66 (2017) 235–250
March

Removal of non benzidine direct red dye from aqueous solution by using natural sorbents: *Beech* and *Silver Fir*

Simona Gabriela Muntean[a,*], Anamaria Todea[a], Snejana Bakardjieva[b], Cristian Bologa[c]

[a]*Institute of Chemistry Timisoara of Romanian Academy, 24 Mihai Viteazul Av., 300223 Timisoara, Romania; Tel. 0040724634237, Fax 0040256191824, email: sgmuntean@acad-icht.tm.edu.ro (S.G. Muntean), anamaria.todea@upt.ro (A. Todea)*
[b]*Centre of Instrumental Technique, Institute of Inorganic Chemistry, Academy of Science of Czech Republic, Husinec-Řež 1001, 250 68 Řež, Czech Republic, Tel. 266173141, email: snejana@iic.cas.cz (S. Bakardjieva)*
[c]*University of New Mexico, Albuquerque, 8713, USA, email: cbologa@salud.unm.edu (C. Bologa)*

Received 3 February 2016; Accepted 18 June 2016

ABSTRACT

The capacity of natural sorbents to remove direct dye from synthetic wastewater has been investigated. Two wood samples (*Beech* and *Silver fir*) were chosen to be tested for the removal of a direct red dye (*DR*). The effects of the support nature, dose, the specific surface of natural fibres, as well as the dye concentration, temperature and the pH influence on the adsorption process were investigated. The results indicate that the percentage of the removed dye rises with reducing the temperature and increasing the dose of the natural fibre, by reducing the apparent area of the sorbent. The kinetics of adsorption obeys a pseudo-second-order rate equation, and Sips isotherm models were found to fit the experimental results the best. The thermodynamic analysis shows that adsorption of *DR* on the investigated wood fibres was favourable and spontaneous.

Keywords: Direct Red; Silver fir; Beech; Adsorption; Kinetics

1. Introduction

The tinctorial process represents an important step in the textile finishing technologies. It has been estimated that more than 10–15 % of the total dyestuff used in dye manufacturing and textile industry is released into the environment during their synthesis and dying process [1]. Pollution in the tinctorial process is determined, by the presence of dyes as chemicals (i.e. eco-toxicological characteristics), and the presence of colour, which itself has features that affect the environment. Insignificant quantities of colouring (the order of 1 mg L^{-1}) may cause an abnormally coloration of water courses, which alert the public opinion [2,3]. Direct dyes, widely used for dyeing textiles and leather, have a complex aromatic structure, which makes them more stable and hardly biodegradable. The potential toxicity of direct dyes arises from the reduction of the azo group, under the action of the enzymes and intestine microflora, which can produce carcinogenic, and mutagenic aromatic amines [4–6]. For these reasons one of the biggest environmental problems is the removal of synthetic dyes from wastewater. The problem of purification of wastewater has both an economic aspect (product recovery, and reuse of recycled water), as well as a health issue, in order to avoid a potentially hazardous water impurity [7,8].

Several physical or chemical methods were reported up to now for treatment of colour wastewater: electrochemical reduction [9], biodegradation [10], chemical oxidation [11], coagulation [12], ultra-filtration [13], and adsorption [14–17]. Among them, adsorption process provides an attractive alternative for the treatment of dye-contaminated waters due to its simplicity, selectivity and efficiency [18]. In the recent years, dye adsorption studies have been focused on natural polymers and their derivatives (peat, chaff [19], sawdust [20], chitosan [14], cyclodextrin [21], bark, wood [22], algae), and biomass (bacteria, fungi) [5], uses as supports for removal of the

---

*Corresponding author.

dyes from wastewaters. On the contrary to the chemical oxidation processes, adsorption technique does not lead to the formation of harmful by-products [23]. The most used adsorbent to remove pollutants from waters is activated carbon [24–28]. Due to the higher cost of activated carbon, the use of this adsorbent is limited. Instead of activated carbon, natural clays such as sepiolite, vermiculite, bentonite, etc. have been used as adsorbents with low cost and high adsorption efficiency [23,29]. Attention has focused on various natural solid supports, which are able to remove pollutants from contaminated water with minimal cost.

Great quantities of sawdust and shavings (by products) are produced annually by the wood industries. Although many outlets are available for the utilization of wood fines, economical disposal of sawdust, and shavings remains a problem of growing concern to the wood industry [30]. At the same time, the vegetal origin textile fibres consist one of the most important group of materials with similar behaviour in tinctorial process and great practical applications.

Silver fir and *Beech* are abundant by-products of sawmills, so they are easily available at negligible price. It contains various organic compounds (lignin, cellulose and hemicellulose) with polyphenolic groups, and due to their physico-chemical characteristics, they could by valorise as low cost sorbents [31,32].

The purpose of this study was the experimental and theoretical investigation of the adsorption of a direct dye (*DR*) from aqueous solutions using natural sorbents. Two types of natural cellulose fibers—*Silver fir* and *Beech*, were tested as sorbents. The effect of process variables such as dye concentration, pH, and temperature has been investigated. The kinetic rate constants and the thermodynamics characteristic parameters of adsorption have been calculated.

2. Experimental

2.1. Materials

The adsorption of a disazo dye derived from 4,4′-diaminobenzanilide, previously synthesized [33] onto cellulose fibre was investigated.

Silver fir (*Abies alba*) is a wood fibre moderately soft and white which contain only wooden vessels (parenchyma). It is used for general construction and paper manufacture [34]. *Beech* wood (*Fagus sylvatica*) is primarily reddish-brown in color with medium stiffness and resistance to shock, and excellent bending characteristics [35]. Wood samples in form of shavings were purchased from the local wood processing industry, the Gref Forest S.R.L. Company, Romania. These samples resulted from wood processing, and could be reused without additional costs.

2.2. Methods

Wood samples were washed in distilled water under constant stirring for 2 h to release impurities, filtered, and then dried in an oven at 60°C for 24 hours, prior to the adsorption studies.

100 mL dye aqueous solutions were treated with two types of natural sorbents. The mixture was kept under magnetic stirring (250 rpm), at different working conditions (temperature, pH), a sufficient and necessary time for reaching the equilibrium.

The obtained specifically sorbent was separated by filtration, washed twice with 50 mL distilled water, and dried at 313 K.

Scanning electron microscopy (SEM) was used for the structural characterization of the studied fibres, before and after dye adsorption, using PHILIPS XL 30 CP scanning microscope, in low vacuum module. Apparatus details: accelerating voltage 300 kV, cathode LaB_6, point-to-point resolution 0.17 nm, line resolution 0.14 nm objective lens, Cs 0.6 mm objective lens, Cc 1.3 mm tilt ± 20.

The dye concentration in solution at initial time (t_0) and at time *t* was spectrophotometrically determined, using a CECIL CE 7200 Spectrophotometer.

The obtained data were used to calculate the adsorption capacity (q_t) based on relation (Eq. (1)), and the dye removal percentage (η) with relation (Eq. (2)).

$$q_t = \frac{(C_0 - C_t)\cdot V}{W} \tag{1}$$

where: q_t is the quantity of dye absorbed per unit mass of dry sorbent (mg g^{-1}), C_0 is initial concentration of the dye solution (mg L^{-1}), C_t is the dye concentration at different periods of time (mg L^{-1}), *V* is the volume of solution (L), and *W* is the amount of sorbent (g).

$$\eta = \frac{(C_0 - C_e)}{C_0}\cdot 100 \tag{2}$$

where C_e is the dye concentration at equilibrium (mg L^{-1}).

3. Results and discussion

The chemical structures and the main characteristics of the non-benzidin *DR* (Direct Red) dye are presented in Table 1. The dye was previously synthesized by our group, by the direct bisdiazotisation of 4,4′-diamino-benzanilide, and two coupling reactions of the resultant bis-diazonium salt with different coupling components: salicylic acid and benzoyl I acid. The dye was then characterized by UV-Vis spectroscopy, thin layer chromatography, and mass spectroscopy [29]. The toxicity of the synthetized dyes was evaluated by biological tests, and the results indicate that these dyes exhibit toxicity values lying in a low scale of toxicity [36,37].

Based on the characterization methods, the structural characteristics of the direct dye: linearity, oblong shape of molecule, coplanarity of molecule, the presence in molecule of soluble groups were demonstrated. Regarding the chemical structure of the selected dye mainly the functional groups capable to establish hydrogen bonds with cellulose fibre the sorbent capacity was investigated.

The chemical compositions of the wood sample include mainly biopolymers such as cellulose, lignin and hemi-

Table 1
The direct *DR* dye characteristics

DR dye structure	Molecular weight (g mol^{-1})	λ_{max} (nm)	$E_{1cm}^{1g/l}$ (CH$_3$COONa 1%)
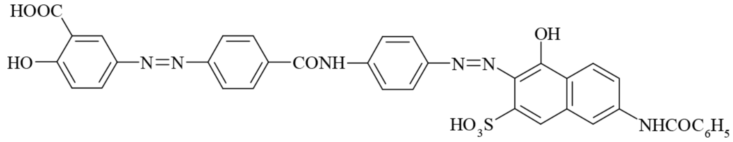	730.72	507	43.4

celluloses. The amount of these polymers varies function of wood nature: resinous or broadleaf respectively, that can influence the reactivity, due the presence of hydroxyl groups in the polymer chain. The cellulose amount in the tested samples used in this study could range up to 55% in *Silver fir* and up to 50% in *Beech*, hemicelluloses 24–40% *Silver fir*, 25–35 % *Beech* and lignin up to 25% in *Silver fir* samples and up to 35% in *Beech* samples [38].

The morphology of the wood samples was investigated by SEM. In Fig. 1 are presented the SEM images of the wood samples before (a, b), and after dyeing with *DR* dye (c, d). In the case of *Silver fir* sections (Fig. 1a), are visible almost exclusively type timber vessels predominantly dotted traheides, strongly lignified. In case of *Beech* (Fig. 1b) elongated cells of timber vessels, with thickening of various types (spiral, reticulated, dotted), and tissue elements of wood–wood fibre and wood parenchyma can be observed. Thus, all of the items in the trunk wood tissue of trees are lignified.

After extracting the final solution, the colored *Silver fir* and *Beech* fibers (Fig. 1—*Supplementary material*) were washed with distilled water and then dried at room temperature.

The SEM photographs of the colored fibers (Fig. 1c,d) showed a uniform and persistent coloration of the samples, and no texture or shape modifications of the original wood fibers were observed after dye adsorption process.

Considering that the samples are composed of plant tissues with cell walls impregnated with lignin, it could not be set a possible selective affinity of dyes to cellulose and

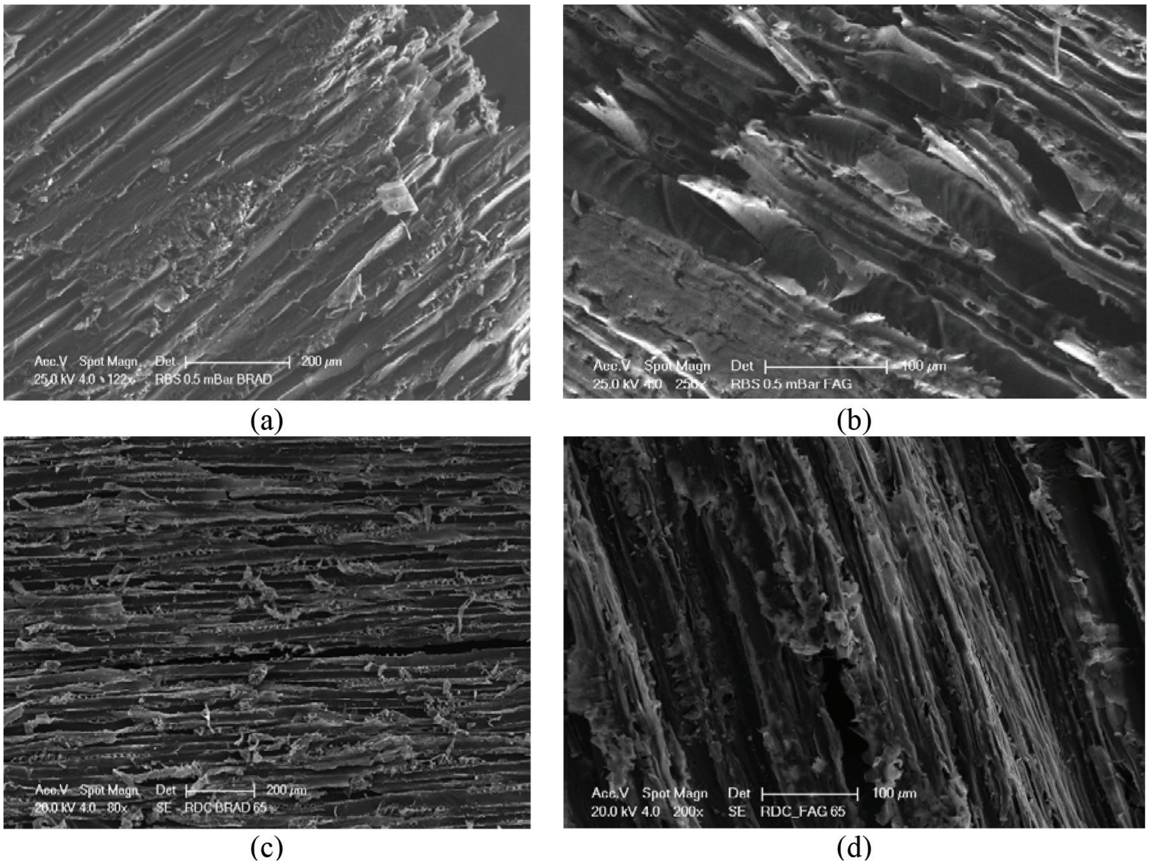

Fig. 1. SEM images for: (a) *Silver fir* fiber; (b) *Beech* fiber; (c) *Silver fir* with *DR* dye; (d) *Beech -DR* dye.

lignin. A possibility to establish the dyes affinity onto different functional groups of the studied wood samples could be represented by performing the adsorption process onto different vegetal tissues from sections of the stems of herbaceous plants. In order to this, *DR* dye was dissolved in distilled water and applied onto stem sections of the pumpkin (*Cucurbita Pepo*). No important differences were observed that indicate probably a lack of selectivity of the investigated dye for present plant tissues.

3.1. Effect of pH on adsorption

The adsorption of the selected dye on the wood materials was previously tested by our group [39], and due to the promising results, the study was completed for this report.

The pH plays an important role for the adsorption process and particularly on the adsorption capacity. The degree of dye adsorption to the sorbent surface is primarily influenced by the surface charge on the sorbent, which is influenced by the pH of the solution.

The experiments were performed by using dye solution (15.48 mg L^{-1}) at different pH values in the range of 3 and 12 (adjusted with CH$_3$COOH or Na$_2$CO$_3$), in seven levels, at 318 K. After the pH adjustments, the samples were placed into the oven (303 K) over night; and the adsorption analyses were performed afterwards.

The maximum adsorption capacity was recorded at low pH (3.5), while at higher pH value (11.3) the sorption of *DR* dye was not effective (Fig. 2). The direct *DR* dye is negatively charged in solution (–SO$_3^-$, –COO$^-$), having an affinity to materials with positive charges. On the other hand, at low pH values, the concentration of H$^+$ ions increases, and the surface of the wood samples become positively charged, while at high pH value, the number of hydroxyl groups increases, so the electrostatic repulsion occurs due to number of negatively charged sites on the sorbent [40] Similar trends were observed by Dulman and Cucu [22], and Khan et al. [41].

Although the higher absorption capacities were obtained in acidic medium, the possible structural modifications of the wood samples (partial hydrolysis and hemicelulose solubilization, redistribution of lignin on fiber surface) at lower pH values should be taken in account [42]. In order to avoid this effect, the following adsorption studies were performed at pH 6.8, the native pH value of the *DR* aqueous solution.

3.2. Influence of the support nature

The adsorption capacity of the sorbent materials is influenced by the nature of the support, the chemical structure of the support, and the number of functional groups able to interact with the dye.

In this study the adsorption capacities of the two natural materials (*Silver fir*, *Beech*) in the *DR* dye removal process were investigated. The experiments were conducted using 0.1 g sorbent in 100 mL of dye aqueous solutions (77.4 mg L^{-1}) under magnetic stirring, at 318 K, and pH 6.8.

The results indicate a retention capacity of *Silver fir* two times higher than the adsorption capacity of *Beech* sawdust (Fig. 3 and Table 3)

The efficiency and capacity of the natural fibres in dyes removal are highly dependent of the differences in chemical composition and the structure and granularity of the wood fibres between the two tree species [43].

3.3 Effect of natural fibre dosage

The influence of the quantity of wood samples towards the dye adsorption was studied at different quantities of natural supports (0.1 and 0.2 g), in 100 ml dye solution using an apparent area of fibre 1.0 cm^2, pH 6.8, 318 K. The results (Table 3, Fig. 2—*Supplementary material*) indicate that the quantity of dye absorbed per unit of dry sorbent decreased, and the efficiency of the dye adsorption increased when the weight of fibre was doubled. This is due to the higher amount of dye per unit weight of fibre, attributed to increase of the number of adsorption sites [44]. The obtained results indicate that the efficiency of the tested wood samples is time dependent and increased in the following order: (*Beech* > *Silver fir*).

As we expected the necessary time for reaching the equilibrium decreased with increasing the quantity of used fibre.

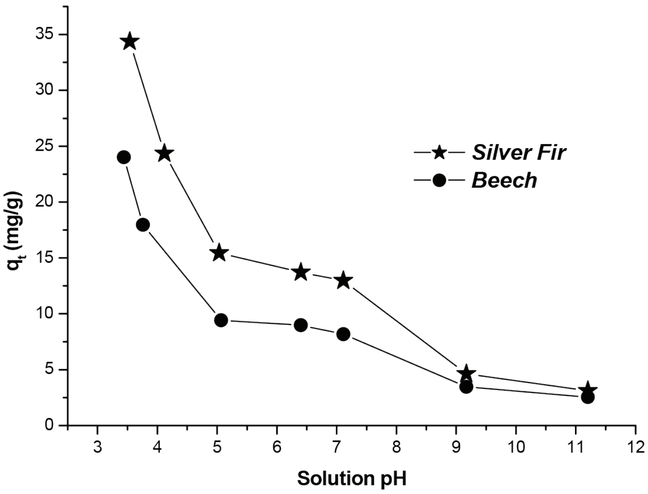

Fig. 2. The effect of pH onto *DR* dye removal.

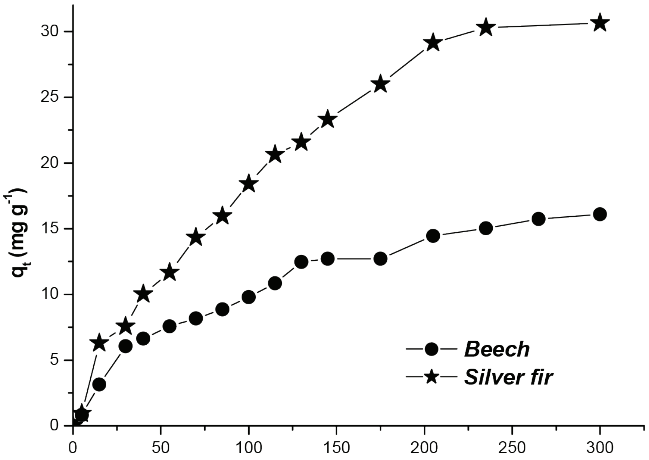

Fig. 3. Influence of the support's nature on to amount of adsorbed *DR* dye (dye concentration 77.4 mg L^{-1}, 1g L^{-1}, 318 K, pH 6.8).

Table 2
Adsorption of *DR* dye on different natural supports type

Dye	Support	$m_{sorbent}$ (g L^{-1})	Apparent support area (cm^2)	t_e (min)	*q* (mg g^{-1})	η* (%)
DR	*Beech*	1	1	260	16.08	20.78
		2	0.5	265	16.63	42.98
			1	240	10.70	27.65
	Silver fir	1	1	235	30.66	39.61
		2	0.5	250	24.92	64.40
			1	220	17.06	44.09

3.4. Effect of sorbent specific surface

The effect of specific surface on the dye removal was investigated for 0.5 and 1 cm^2 respectively, under constant experimental conditions, and the results are presented in Table 3 and Fig. 3—*Supplementary material*. The quantity of dye absorbed per unit of dry sorbent and the removal percentage decrease (from 16.08 to 10.7 mg g^{-1} in case of *Beech*, and from 30.66 to 17.06 mg g^{-1} in case of *Silver Fir*) when the weight of fibre was doubled indicating that adsorption process works better for small geometric dimensions. The same effect was observed by Ho [45]. The observed effect could be appear due to the increase of accessibility of sorbent surface area with the decrease in specific surface, which allows more dye molecules to be adsorbed per unit of substrate.

By reducing the sorbent area, the specific area between the phases involved in the transfer, and also the number of available adsorption sites was increased, so physicochemical operations were facilitated and hurried. The adsorption capacity as well as removal percentage were about 1.5 times higher when sorbent samples with smaller support area were used.

3.5. Influence of initial dye concentration

For ecological reasons, recovery of dyes from diluted colored wastewater is very important. The effect of initial dye concentration on the adsorption capacity of *Silver fir* and *Beech* was investigated using four different concentrations in the range 7.74–77.4 mg L^{-1}, at 318 K, and pH 6.8.

The results presented in Fig. 4 and Table 4 indicates that the *DR* dye removal was rapid at the beginning of the adsorption process, and gradually decreased as equilibrium time was approached, due to the saturation of the active centre, available for dye on the sorbents surface. The necessary time to reach the equilibrium increased with increasing the dye concentration, due to the fact that adsorption could occur both at the surface, and in the pores of the sorbent, and the diffusion into the internal adsorption sites is stimulated by the increasing of the initial dye concentration.

By increasing the initial dye concentration, the amount of dye adsorbed increased in both cases, while the percentage removal decreased, indicated that the dye removal is concentration dependent, which is in agreement with data obtained by Dulman [22], and Şener [46].

3.6. Influence of temperature on the adsorption process

In order to explain the effect of temperature on the dye adsorption, the experiments were conducted at pH 6.8, using 77.4 mg L^{-1} dye concentration, and three temperature values (303, 318, and 333 K). The calculated q_t values (at the chosen values of temperature) depicted in Fig. 5, indicate that the adsorption of *DR* decreases as the solution temperature increases probably due to the increase of the entropic factors.

Also the exothermic characteristic of the adsorption process and the weakening of bonds between dye molecules and active sites of sorbents at high temperatures is a possible explanation of these results. Similar results were obtained by various authors for the adsorption of dyes on various sorbents [47–49].

3.7. Adsorption kinetics

The adsorption kinetics of *DR* dye on two types of sorbents has been investigated under different conditions. The concentration values of dye solutions were determined at certain time intervals during the adsorption process. The

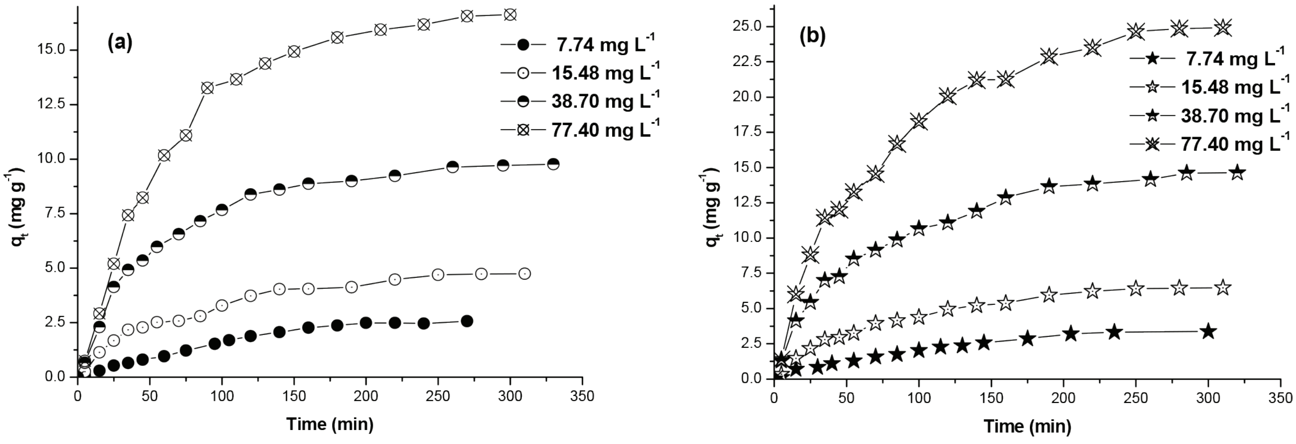

Fig. 4. The effect of initial concentration on *RD* dye removal; (a) *Beech*, (b) *Silver Fir*.

Table 4
Influence of the process variables on the adsorption capacity of investigated sorbents

Dye concentration (mg L^{-1})	q_e (mg g^{-1})		η (%)	
	Beech	*Silver fir*	*Beech*	*Silver fir*
7.74	2.57	3.37	66.44	87.14
15.48	4.75	6.47	61.34	83.63
38.7	9.77	14.63	50.49	75.62
77.4	16.63	24.93	42.98	64.40
Temperature				
(K)				
303	18.61	27.94	48.08	72.19
318	16.63	24.92	42.98	64.40
333	14.11	21.50	36.45	55.57

experimental results obtained for the influence of temperature were analyzed using pseudo first-order Lagergren model (Eq. (3)), pseudo second-order model (Eq. (4)) and intraparticle diffusion model (Eq. (5)) [50].

$$\log(q_e - q_t) = \log q_e - \frac{k_1}{2.303}t \tag{3}$$

$$\frac{t}{q_t} = \frac{1}{k_2 q_e^2} + \frac{1}{q_e}t \tag{4}$$

$$q_t = k_i t^{0.5} + l \tag{5}$$

where: k_1 is Lagergren rate constant (min^{-1}), k_2 is rate constant for the pseudo-second order adsorption model (g mg^{-1} min^{-1}), k_i is the intraparticle diffusion rate constant (mg g^{-1} min$^{-0.5}$) and l is a constant (mg g^{-1}) that gives idea about the thickness of the boundary layer.

The correlation coefficients were used to determine the best fitting kinetic model. The comparison of experimental adsorption capacities values (obtained at different temperature) and the theoretical values, and the computed results estimated from Eqns. (3) and (4), are presented in Fig. 6–8.

The adsorption kinetics data for the influence of concentration on the adsorption process are presented in Table S1 and Figs. 4–6 in *Supplementary materials*.

The best fits were obtained with the pseudo-second order kinetic model and the calculated q values ($q_{e,calc}$) from the pseudo-second-order model show the best agreement with the experimental q values ($q_{e,exp}$). As the temperature increases, the k_2 constant decreases [51], indicating that the necessary time for reaching the equilibrium decreases with increasing temperature, and that the adsorption of *DR* on *Silver fir* and *Beech* is an exothermic process.

Fig. 8 presents the amount of *DR* adsorbed versus $t^{0.5}$ at different temperature. The plots present multilinearity indicating that more steps occur in adsorption processes. The first linear portion is the fastest step attributed to the external surface adsorption of dye. The second linear portion corresponds to intraparticle diffusion, and the third step is the equilibrium stage when diffusion through small pores occurs. The straight line of the intraparticle region at different temperatures does not through the origin indicating that the intraparticle diffusion is not the only rate controlling step [52]. The deviation from the origin may be due to the variation of mass transfer in the initial and final stages of adsorption process [53].

The values of k_i and l obtained from the slope of the straight lines are presented in Table 5. The obtained results demonstrate that the surface diffusion and the intra-particle diffusion occur in parallel during the adsorption process of *DR* dye at different temperatures.

3.8. Equilibrium isotherms

Dyeing is a complex process, although it was extensively studied, it was not satisfactory explained yet. The adsorption of the dye on the internal surface of the fibre is the most important step of the process [54], dyeing being influenced by the nature and the magnitude of dye-fibre intermolecular forces, which affect the dye-fibre affinity. Some authors sustain that adsorption is a monomolecular process; while other authors demonstrated that it is a dif-

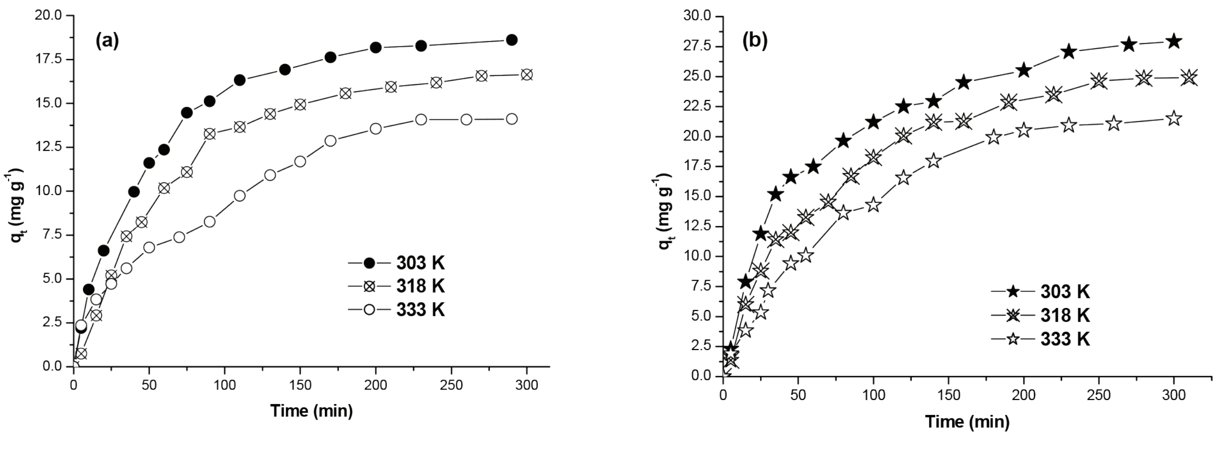

Fig. 5. Effect of temperature on uptake of *DR* on: (a) *Beech* fibre (b) *Silver Fir* fibre (dye concentration 77.4 mg L^{-1}, 1 g L^{-1}, pH 6.8).

Table 5
Comparison of experimental and calculated q_e values, and adsorption rate constants for adsorption of *DR* dye on different sorbents.

Sorbent	Temp. (K)	$q_{e,\exp}$ (mg g^{-1})	Pseudo-first order kinetic model		Pseudo-second order kinetic model		Intraparticle diffusion	
			$q_{e,\text{calc}}$ (mg g^{-1})	$k_1 \cdot 10^3$ (min^{-1})	$q_{e,\text{calc}}$ (mg g^{-1})	$k_2 \cdot 10^4$ (g mg^{-1} min^{-1})	k_i (mg g^{-1} min$^{-0.5}$)	l (mg g^{-1})
Beech	303	18.61	17.29	17.55	19.69	11.00	1.75	–1.10
	318	16.63	18.39	17.13	17.78	9.66	1.55	–2.16
	333	14.11	22.79	21.49	15.61	7.94	1.19	–2.78
Silver fir	303	27.94	22.65	14.53	30.59	6.75	1.86	7.28
	318	24.92	31.57	17.55	28.10	5.36	1.77	0.36
	333	21.50	24.61	15.41	23.93	3.74	1.64	–1.68

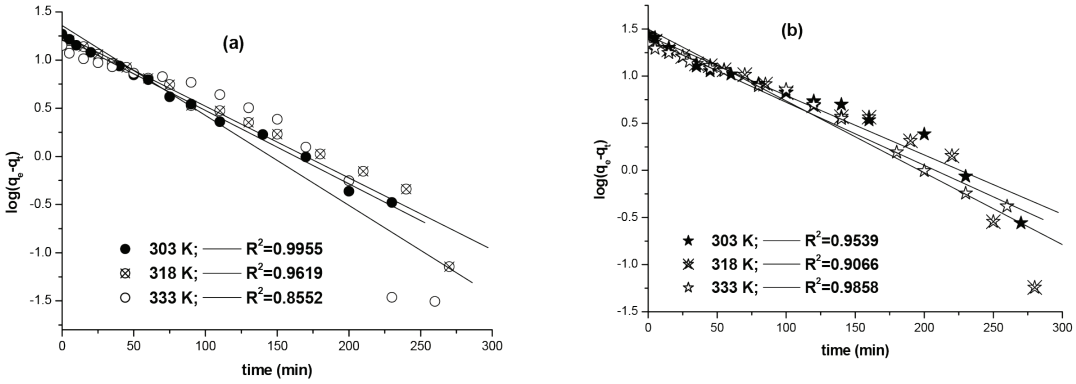

Fig. 6. Lagergren plot for the adsorption of *DR* dye on: (a) *Beech*; (b) *Silver fir* fibre.

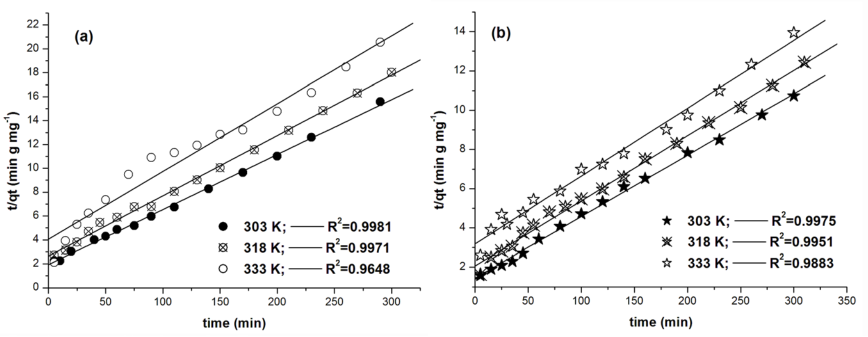

Fig. 7. Pseudo-second-order kinetic model fitting for the adsorption of *DR* dye on: (a) *Beech*; (b) *Silver Fir*.

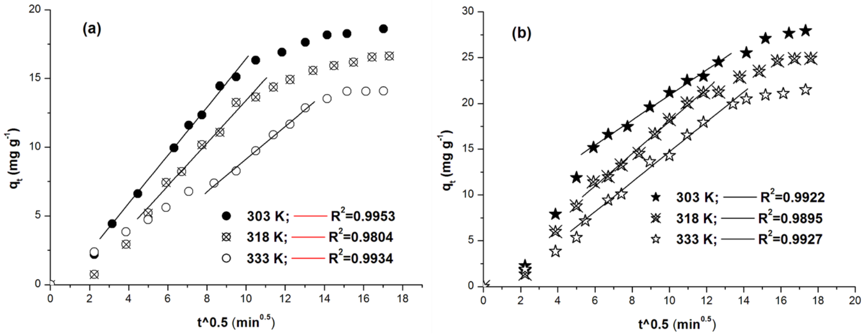

Fig. 8. Intraparticle diffusion model fitting for the adsorption of *DR* dye on: (a) *Beech*; (b) *Silver Fir*.

fuse process, in multiple layers. The adsorption isotherms describe the way in which dyes interact with sorbents. The experimental data were fitted to the theoretical adsorption isotherms Freundlich, Langmuir, Sips, Redlich Peterson, and Dubinin-Raduskevich [55,56].

The analysis of the experimental data and parameters determination that describes the theoretical models were performed by the ORIGIN version 6.1 program, and principal statistical criteria were the standard deviation (SE) and the squared multiple regression coefficient (R^2).

Based on the lower error obtained, the best isotherm model that fits the experimental data was the Sips isotherm model (Table 7). These results suggest that the adsorption process of investigated dye is following a combined model Frendlich and Langmuir: diffused adsorption at low dye concentration, and a monomolecular adsorption with a saturation value—at high dye concentrations.

From the obtained curves the maximum adsorption capacity and the characteristic parameters of Sips equation on investigated sorbents were determined (Table 8); the obtained results are higher or comparable with other published data (Table 9). Based on the higher adsorption capacity obtained in this study by using untreated sawdust (especially *Silver fir*), it could represent an alternative and attractive method for removal of direct dyes from wastewater at low operational cost.

As expected (adsorption is generally exothermic) the equilibrium constant (Ks) decreases with temperature increasing, which can be explained because at higher temperature, increases the stored energy in different types of motion allowed, and weaken the physical binding forces of adsorbed molecules.

Table 6
The adsorption isotherms models

Isotherm	Equation
Freundlich	$q_e = K_F C_e^{1/n}$
Langmuir	$q_e = \frac{q_m K_L C_e}{1+K_L C_e}$
Sips	$q_e = \frac{q_m K_S C_e^{1/n}}{1+K_S C_e^{1/n}}$
Redlich-Peterson	$q_e = \frac{K_{RP} C_e}{1+\alpha_{RP} C_e^{\beta}}$
Dubinin-Raduskevich	$C_f = S_f \cdot e^{-B\varepsilon^2} \varepsilon = RT\ln\left(1+\frac{1}{C_S}\right)$

The results for the parameter *n* are lower than 1, indicating that the heterogeneity degree of the studied systems is very small. *n* practically does not vary with temperature, and does not depend on the sorbent material.

For a better description of adsorption equilibrium at different temperatures, it is important to have the dependence form of the Sips equation. The temperature dependence of the Sips equation is given by equations:

$$K_S = K_0 \cdot \exp\left[\frac{Q}{RT_0}\cdot\left(\frac{T_0}{T}-1\right)\right] \tag{11}$$

$$n = \frac{1}{\frac{1}{n_0}+\beta\cdot\left(1-\frac{T_0}{T}\right)} \tag{12}$$

$$S_f = S_{f0}\cdot\exp\left[\chi\cdot\left(1-\frac{T}{T_0}\right)\right] \tag{13}$$

where: K_S is the Sips constant related with affinity constant, χ and β are coefficients that take into account: χ the temperature dependence of the maximum concentration of adsorbed sorbent ($S_{f\,0}$), β the temperature dependence of the Sips parameter in the equation. Constant *n* is a parameter which characterizes the heterogeneous nature of the system [67].

The optimal parameters of the Sips equation (Table 9) were obtained by simultaneously fitting the experimental values obtained for three temperatures, using multiparametric nonlinear regression module. Experimental results and simultaneous fitting with Sips equation are presented in Fig. 9.

The shape of the isotherms leads to the idea that after Brunauer's classification, they are of type V (sigmoid shape). The explication for this shape is that at the studied temperatures, the monolayer adsorption of the dye (there is a saturation concentration of each) must be preceded by dissociation of the formed aggregates in solution. Indeed, the tendency to form sigmoid shape is pronounced in case of *DR* dye isotherms which form dimmers [68]. Therefore, the results of thermodynamic equilibrium are influenced by aggregation, which overlaps with the dyeing equilibrium.

Tabel 7
The squared multiple regression coefficient values obtained by fitting of different isotherms to the adsorption experimental data

Dye	Sorbent	Temperature	R^2				
		(K)	Freundlich	Langmuir	Sips	Redlich-Peterson	Dubinin-Radushkevich
DR	*Beech*	303	0.9245	0.9462	0.9964	0.9462	0.9407
		318	0.9247	0.9476	0.9959	0.9476	0.9409
		333	0.9227	0.9576	0.9922	0.9576	0.9402
	Silver fir	303	0.8715	0.9143	0.9980	0.9143	0.8931
		318	0.8966	0.9358	0.9983	0.9358	0.9162
		333	0.9014	0.9301	0.9971	0.9288	0.9184

Table 8
Sips equation parameters

Dye	Sorbent	Temp. (K)	S_f (mg g^{-1})	n	K_S (L mg^{-1})	R^2
DR	*Beech*	303	22.84	0.339	0.030	0.9969
		318	18.26	0.379	0.029	0.9968
		333	13.98	0.345	0.026	0.9942
	Silver Fir	303	34.20	0.340	0.031	0.9985
		318	27.35	0.363	0.030	0.9979
		333	20.87	0.338	0.028	0.9978

Table 9
Adsorption capacities of different natural/low cost sorbent for the uptake/adsorption of direct dyes from its aqueous solutions

Adsorbate	Sorbent	Adsorption capacity q_t (mg g^{-1})	Reference
Direct Orange 26	Beech	2.78	[57]
Congo Red	*Leucaena leucocephala* seed pods	4.41	[58]
Methylene blue	Fir	6.45	[59]
Reactive Red 195	*Pynus sylvestris* L.	7.35	[60]
Basic Red 46	Fir	20.47	[61]
	Beech	19.24	
Direct Red 23	Mangrove barks	21.55	[62]
Egacid Orange	Spruce wood	24.22	[63]
Red Reactive 141	Wood-shaving ash	24.30	[64]
Acid Blue 25	*Shorea dasyphylla* sawdust	24.39	[65]
Direct Red 28	*Syzygium cumini*	29.79	[66]
Direct Red	Silver Fir	34.20	This study
	Beech	22.84	
Direct Blue 53	Cupuassu shell	37.50	[44]

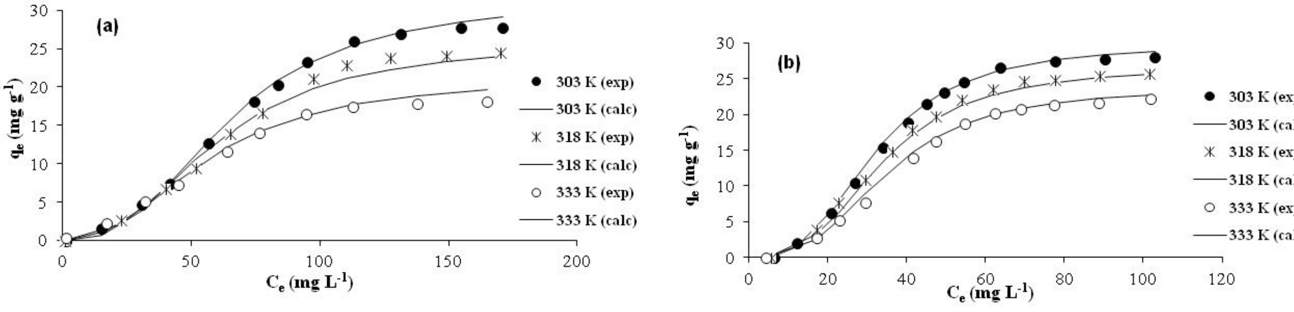

Fig. 9. Sips plots for the adsorption of *DR* dye on (a) *Beech*, (b) *Silver fir* fibre.

The χ parameter values for the investigated fibres are significantly different by zero. This is not surprising, given that wood is immersed in solution (water) and at different temperatures probably changes its hydration degree. It is well known that wood is an anisotropic material, the thermal expansion coefficient depending on the investigated direction [69]; this type of anisotropy can affect the ratio of "micropores, mesopores and macropores" from sorbent. This property leads to changes in the number of active adsorption centers with temperature variation, probably by modifying the internal porous structure.

Constant β values for the studied systems are practically negligible. This means that, for the investigated temperature range, the heterogeneity degree does not vary with temperature.

The adsorption energy values (Q) representing the energy barriers of desorption, are in the range of 2200, and respectively 3400 J mol^{-1}. These values do not allow decid-

Table 10
Parameters of Sips equation

Parameter	*DR*	
	Beech	*Silver fir*
S_{f0} (mg g^{-1})	30.87	33.41
χ	3.83	2.22
K_0 (L mol^{-1})	11450.90	23857.21
Q/RT_0	1.474	0.972
Q	3345.57	2206.17
n_0	0.37	0.339
β	0.079	0.017
R	0.9962	0.9982

ing what type of intermolecular interactions occurs in the studied systems.

Hartono et al. showed that liquid phase adsorption of organic compounds on porous solid sorbents is affected by several factors such as: molecular weight, polarities of the sorbent-adsorbate, and orientation of the adsorbed molecules on the sorbent surface [49]. In Table 11 are presented some structural parameters (descriptors) proportional to molecule size and shape, and with capacity to interact with the sorbent.

The obtained values (Table 10) allow us to draw the following conclusions: the adsorption capacity of *Silver Fir* is higher than that of *Beech*, so we can affirm that the number of adsorption active centres decreases in the same order. Table 11 appears several descriptors vary in the same order: the globular factor (1 for spherical molecules) shows that *DR* is a compact molecule, which can access the smaller pores of the sorbent. Amount of the main moments of inertia, $I_x + I_y$, is appreciatively equal with I_z which means that molecules are approximately planar, the molecules steric requirements in 3D space means that are proportional to I_y, and I_z. These results suggest that the pore size plays an important role in the adsorption of *DR*, a dye with relatively large molecule.

Table 11
The structural parameters for investigated dye

Parameter/dye	*DR*
Molar mass (g mol^{-1})	737.2
Molecule volume (Å^3)^a	1782.95
Molecular surface (Å^2)^b	582.49
Solvent accessible molecular surface (Å^2)^{b,d}	1009.43
Volume excluded from contact with solvent (Å^3)^{b,d}	502.28
Polar molecular surface (Å^2)^c	248.15
Principal moments of inertia, Iz (g mol^{-1}• Å^2)^b	64896.8
Principal moments of inertia, Ix + Iy (g mol^{-1}• Å^2)^b	65005.29
Index oval^b	1.906
Globular factor (1/index oval)	0.525
Hydration energy (kJ mol^{-1})^a	–128.74
ClogP (calculated octanol/water partition coefficient)^b	7.202
Number of hydrogen-bond donor (pH = 4 ÷ 9)^c	4
Number of hydrogen-bond acceptor (pH = 4 ÷ 9)^c	13

[a] Calculated with the software package HyperChem
[b] Calculated with the software package Chem3D Ultra, http://cambridgesoft.com
[c] Calculated with the software package (online) Marvin, http://www.chemaxon.com./marvin/sketch/index.jsp

ClogP parameter (proportional to molecules hydrophobicity) indicates that the dominant intermolecular interaction for *DR* dye is nonpolar (van der Waals).

The obtained results for Sips model were used to calculate the thermodynamic parameters for the adsorption process. The Gibb's free energy change (ΔG^0), was calculated using equation (Eq. (14)):

$$\Delta G^0 = -RT\ln K_S \tag{14}$$

and enthalpy change (ΔH^0), and entropy change (ΔS^0) was determined from van't Hoff equation:

$$\Delta G^0 = \Delta H^0 - T\Delta S^0 \tag{15}$$

where: *R* is the universal gas constant (8.314 J K^{-1} mol^{-1}), *T* the absolute temperature, and Ks represents the Sips equilibrium constant, obtained from the isotherm plots. ΔH^0 and ΔS^0 values can be calculated from the slope and intercept of the linear plot of lnK_s versus $1/T$.

The obtained negative values of ΔG^0 indicate the spontaneous nature of the adsorption process. The increase of temperature determined a decrease of ΔG^0 indicating that adsorption is facilitated by lower temperatures. The negative values of ΔH^0 reveal an exothermic nature of adsorption. The positive value of entropy reflects the increased randomness at the solid-solution interface. According to Boltzmann's theory, entropy is proportional to the system probability. In terms of dyeing, the change in entropy has practical importance when we compare the performance of two (or more) sorbents. The ΔS^0 values show that for the *DR-Silver fir* system the binding is more rigid (lower entropy), and the *DR- Beech* system is less (higher entropy).

Table 12
Thermodynamic parameters for the adsorption of *DR* on *Beech* and *Silver Fir*

Dye	Sorbent	Temp. (K)	ΔG^0 (J mol^{-1})	ΔH^0 (J mol^{-1})	ΔS^0 (J mol^{-1} · K^{-1})
DR	*Beech*	303	–23574.86	–19175.08	1448.72
		318	–24862.67		
		333	–26472.29		
	Silver fir	303	–25383.28	–22238.22	1062.91
		318	–26577.15		
		333	–27509.08		

4. Conclusions

In order to remove a direct dye from wastewater we investigate two wood fibers as potential sorbents. The natural sorbents—*Silver fir* and *Beech* were used without any changes, in order to achieve the minimum costs. Better yields were obtained using *Silver fir* shavings (87.14%), compared with using *Beech* shavings (72.19%). Increases of the amount of investigated fibres produced an increased in efficiency, and a decreased of the necessary time for reaching the equilibrium. Also, the adsorption capacity increased with decreasing of the specific surface, solution pH, and the temperature.

The pseudo second-order model was found to be best fitting kinetic models, and the calculated quantity of dye absorbed $q_{\mathrm{e,calc}}$ were in consistent with the experimental values, $q_{\mathrm{e,exp}}$, indicated that chemisorptions plays a role in rate determining step. The results obtained for intra particle diffusion model application demonstrate that the surface diffusion and the intra-particle diffusion occur in parallel during the adsorption process

The experimental data were well correlated by the Sips adsorption model, and the maximum theoretical adsorption capacities determined by simultaneously fitting for three temperatures, were 30.87 mg g^{-1} for *Beech* and 33.41 mg g^{-1} for *Silver fir* respectively.

Thermodynamic analysis demonstrated that adsorption of *DR* dye on *Beech* and *Silver fir* sawdust was favorable and spontaneous (negative values of ΔG^0) exothermic (negative values of ΔH^0) increased disorder and randomness at the solid-solution interface (positive values of ΔS^0).

The lower prices of investigated supports (wastes from wood industries), and the ratio price/performance allow us to propose the shavings *Silver fir* and *Beech* as attractive alternative sorbents for costly activated carbon, for the removal of small amounts of direct dyes (low concentrations) from wastewaters.

Symbols

DR — Direct red dye
q_t — Amount of dye adsorbed onto the sorbent unit at time t (mg g^{-1})
C_0 — Dye concentration in solution at initial time (mg L^{-1})
C_t — Dye concentration in solution at time t (mg L^{-1})
C_e — Dye concentration at equilibrium (mg L^{-1})
V — Solution volume (L)
W — Amount of sorbent (g)
k_1 — Rate constant of pseudo-first order adsorption model (min^{-1})
k_2 — Rate constant of pseudo-second-order adsorption model (g mg^{-1} min^{-1})
k_{i} — Intraparticle diffusion rate constant (mg g^{-1} min$^{-0.5}$)
l — Effect of boundary layer thickness
t — Time (min)
K_F — Constant of Freundlich isotherm (mg g^{-1} (mg L^{-1})$^{-1/n}$))
n — The Freundlich exponent (dimensionless)
K_L — Constant of Langmuir isotherm (L mg^{-1})
K_S — Sips constant related with affinity constant ((mg L^{-1})$^{-1/n}$)
K_{RP} — Constant of Redlich-Peterson isotherm (L g^{-1})
α_{RP} — The Redlich-Peterson constant (mg L^{-1})$^{-\beta}$
β — The Redlich-Peterson exponent (dimensionless) ($0 < \beta < 1$)
q_e — Equilibrium solid phase concentration (mg g^{-1})
$q_{\mathrm{e,cal}}$ — Calculated value of solid phase concentration of adsorbate at equilibrium (mg g^{-1})
$q_{\mathrm{e,exp}}$ — Experimental value of solid phase concentration of adsorbate at equilibrium (mg g^{-1})
q_m — Maximum adsorption capacity of sorbent (mg g^{-1})

Acknowledgement

This work was supported by Program 2 of the Institute of Chemistry Timisoara of Romanian Academy (Research Project 2.4.).

References

[1] K. Sarayu, S. Sandhya, Potential of facultative microorganisms for biotreatment of textile wastewater, Envis Centre Newsletter, 7(2) (2009).
[2] Green chemistry for dyes removal from wastewater, Chapter 11, J. Mittal, A. Mittal, *Hen Feather*, a remarkable adsorbent for dye removal, 2015, 409–457, S.K. Sharma, ed., Scrivener Publishing LLC, USA.
[3] A. Mittal, L. Kurup, Column operations for the removal and recovery of a hazardous dye 'acid red - 27' from aqueous solutions, using waste materials—bottom ash and de-oiled soya, Eco. Env. Cons., 13 (2006) 181–186.
[4] H.M. Pinheiro, E. Touraud, O. Thomas, Aromatic amines from azo dye reduction: status review with emphasis on direct UV spectrophotometric detection in textile industry wastewaters, Dyes Pigments, 61 (2004) 121–139.
[5] G. Bayramoğlu, M. Yarup Arica, Biosorption of benzidine based textile dyes "Direct Blue 1 and Direct Red 128" using native and heat-treated biomass of *Trametes versicolor*, J. Hazard. Mater., 143 (2007) 135–143.
[6] J. Wang, H.S. Freeman, L.D. Claxton, Synthesis and mutagenic properties of direct dyes from 4,4′-diamino-p-terphenyl and 4,4′-diamino-p-quaterphenyl. Color. Techn., 123 (2007) 39–45.
[7] J. Mittal, D. Jhare, H. Vardhan, A. Mittal, Utilization of bottom ash as a low-cost sorbent for the removal and recovery of a toxic halogen containing dye eosin yellow, Desalin. Water Treat. 52(22–24) (2014) 4508–4519.
[8] G. Sharma, M. Naushad, D. Pathania, A. Mittal, G.E. El-Desoky, Modification of *Hibiscus cannabinus* fiber by graft copolymerization: application for dye removal, Desalin. Water Treat., 54(11) (2015) 3114–3121.
[9] G.R. de Oliveira, N.S. Fernandes, J.V. de Meloda, D.R. Silva, C. Urgeghe, C.A. Martínez-Huitle, Electrocatalytic properties of Ti-supported Pt for decolorizing and removing dye from synthetic textile wastewaters, Chem. Eng. J., 168 (2011) 208–214.
[10] C.H. Niebisch, A.K. Malinowski, R. Schadeck, D.A. Mitchell, V. Kava-Cordeiro, J. Paba, Decolorization and biodegradation of reactive blue 220 textile dye by *Lentinus crinitus* extracellular extract, J. Hazard. Mater., 180(1–3) (2010) 316–322.
[11] V.P. Santos, M.F.R. Pereira, P.C.C. Faria, J.J.M. Órfão, Decolourisation of dye solutions by oxidation with H_2O_2 in the presence of modified activated carbons, J. Hazard. Mater., 162(2–3) (2009) 736–742.
[12] B. Shi, G. Li, D. Wang, C. Feng, H. Tang, Removal of direct dyes by coagulation: The performance of preformed polymeric aluminum species, J. Hazard. Mater., 143 (2007) 567–574.
[13] A. Aouni, C. Fersi, B. Cuartas-Uribe, A. Bes-Pía, M.I. Alcaina-Miranda, M. Dhahbi, Reactive dyes rejection and tex-

tile effluent treatment study using ultrafiltration and nanofiltration processes, Desalination, 297 (2012) 87–96.
[14] Ö. Demirbaş, M. Alkan, Adsorption kinetics of a cationic dye from wastewater, Desal. Water Treat., 53(13) 2015, 3623–3631.
[15] N.F. Cardoso, E.C. Lima, I.S. Pinto, C.V. Amavisca, B. Royer, R.B. Pinto, W.S. Alencar, S.F.P. Pereira, Application of cupuassu shell as biosorbent for the removal of textile dyes from aqueous solution, J. Environ. Manage., 92 (2011) 1237–1247.
[16] H. Tang, W. Zhou, L. Zhang, Adsorption isotherms and kinet ics studies of malachite green on chitin hydrogels, J. Hazard. Mater., 209–210 (2012) 218–225.
[17] C. Kannan, K. Muthuraja, M.R. Devi, Hazardous dyes removal from aqueous solution over mesoporous aluminophosphate with textural porosity by adsorption, J. Hazard. Mater., 244–245 (2013) 10–20.
[18] A. Nejibab, D. Joelleb, A. Fadhilaa, G. Sophieb, T.-A. Malikaa, Adsorption of anionic dye on natural and organophilic clays: effect of textile dyeing additives, Desal. Water Treat., 54(6) (2015), 1754–1769.
[19] R. Han, Y. Wang, P. Han, J. Shi, J. Yang, Y. Lu, Removal of methylene blue from aqueous solution by chaff in batch mode, J. Hazard. Mater., 137 (2006) 550–557.
[20] P.K. Malik, Dye removal from wastewater using activated carbon developed from sawdust: adsorption equilibrium and kinetics, J. Hazard. Mater., 113 (2004) 81–88.
[21] G. Crini, Studies on adsorption of dyes on beta-cyclodextrin polymer, Biores. Technol., 90 (2003) 193–198.
[22] V. Dulman, S.M. Cucu-Man, Sorption of some textile dyes by beech wood sawdust, J. Hazard. Mater., 162 (2009) 1457–1464.
[23] O. Duman, S. Tunc, T. Gurkan Polat, Adsorptive removal of triarylmethane dye (Basic Red 9) from aqueous solution by sepiolite as effective and low-cost adsorbent, Micropor. Mesopor. Mater., 210 (2015) 176–184.
[24] O. Duman, E. Ayranci, Adsorption characteristics of benzaldehyde, sulphanilic acid and p-phenolsulfonate from water, acid or base solutions onto activated carbon cloth, Sep. Sci. Technol., 41 (2006) 3673–3692.
[25] O. Duman, E. Ayranci, Attachment of benzo crown ethers onto activated carbon cloth to enhance the removal of chromium, cobalt and nickel ions from aqueous solutions by adsorption, J. Hazard. Mater., 176 (2010) 231–238.
[26] E. Ayranci, O. Duman, Structural effects on the interactions of benzene and naphthalene sulfonates with activated carbon cloth during adsorption from aqueous solutions, Chem. Eng. J., 156 (2010) 70–76.
[27] E. Ayranci, O. Duman, In-situ UV-visible spectroscopic study on the adsorption of some dyes onto activated carbon cloth, Sep. Sci. Technol., 44 (2009) 3735–3752.
[28] O. Duman, E. Ayranci, Adsorptive removal of cationic surfactants from aqueous solutions onto high-area activated carbon cloth monitored by in situ UV spectroscopy, J. Hazard. Mater., 174 (2010) 359–367.
[29] O. Duman, S. Tunc, T.G. Polat, Determination of adsorptive properties of expanded vermiculite for the removal of C. I. Basic Red 9 from aqueous solution: Kinetic, isotherm and thermodynamic studies, Appl. Clay Sci., 109–110 (2015) 22–32.
[30] J.M. Harkin, Uses for Sawdust, Shavings, and waste Chips (Research note FPL; 0208): 45 p.
[31] O. Aksakala, H. Ucun, Equilibrium, kinetic and thermodynamic studies of the biosorption of textile dye (Reactive Red 195) onto *Pinus sylvestris* L., J. Hazard. Mater., 181 (2010) 666–672.
[32] J. Sánchez-Martín, J. Beltrán-Heredia, I.J. Seabra, M.E.M. Braga, H.C.de Sousa, Adsorbent derived from *Pinus pinaster* Tannin for Cationic Surfactant Removal, J. Wood Chem. Technol., 32 (1) (2012) 23–41.
[33] G.M. Simu, S.L. Funar-Timofei, S.G. Hora, W.E. Schmidt, L. Kurunczi, E.N. Sişu, N. Morin, Direct dyes derivatives of 4,4′-diaminobenzanilide. I - The syntesis and study of adsorption isoterms on cotton of a direct disazoic dye with asymmetrical structure, Rev. Chim. Buc, 53(12) (2002) 826–829.
[34] M. Palade,"Botanica farmaceutică", Ed. Tehnică Bucureşti, vol I (1997) 212–221.
[35] G. Wanner, Mikroskopisch-botanisches Praktikum, Thieme Verlag Stuttgart – New York, 121 (2004) 190–199.
[36] G.M. Simu, S.A. Chicu, N. Morin, W. Schmidt, E. Sisu, Direct dyes derived from 4,4′–diaminobenzanilide synthesis, characterization and toxicity evaluation of a disazo symmetric direct dye, Turk. J. Chem., 28 (2004) 579–585.
[37] S.A. Chicu, M. Munteanu, I. Cîtu, C. Şoica, C. Dehelean, C. Trandafirescu, S. Funar-Timofei, D. Ionescu, G.M. Simu, The *Hydractinia echinata* test-system. III: Structure-toxicity relationship study of some azo-, azo-anilide, and diazonium salt derivatives, Molecules, 19 (2014) 9798–9817.
[38] F. Talebina, Ethanol production from cellulosic biomass by encapsulated *Saccharomyces cerevisiae*, PhD thesis, Goteborg, Sweeden, 2006.
[39] S.G. Muntean, P. Sfârloagă, G. Simu, O. Paska, Sorption of a disazo direct dye on FIR (*Albiens Alba*): equilibrium study, The XVI Symposium on analytical and environmental problems, Szeged, Hungary, 28 Oct. 2009, pp/ 305–308.
[40] A. El Nemr, O. Abdelwahab, A. El-Sikaily, A. Khaled, Removal of direct blue-86 from aqueous solution by new activated carbon developed from orange peel. J. Hazard. Mater., 161(1) (2009) 102–110.
[41] S.R. Khan, A. Inayat, A. Rana, Sorption of reactive and acid dyes from aqueous solutions onto sawdust, Bangladesh J. Sci. Ind. Res., 45(1) (2010) 35–38.
[42] H. Jorgensen, J.B. Kristensen, C. Felby, Enzymatic conversion of lignocelluloses into fermentable sugars: challenges and opportunities, Biofuels, Bioprod. Bioref., 1 (2007) 119–134.
[43] L. Laasri, M.K. Elamrani, O. Cherkaoui, Removal of two cationic dyes from a textile effluent by filtration-adsorption on wood sawdust, Env. Sci. Pollut. R., 14(4) (2007) 237–240.
[44] N.F. Cardoso, E.C. Lima, I.S. Pinto, C.V. Amavisca, B. Royer, R.B. Pinto, W.S. Alencar, S F.P. Pereira, Application of cupuassu shell as biosorbent for the removal of textile dyes from aqueous solution, J. Environ. Manage., 92 (2011) 1237–1247.
[45] Y.S. Ho, G. McKay, Kinetic models for the sorption of dye from aqueous solution by wood, Trans IChemE, 76(B) (1998) 183–191.
[46] S. Şener, Use of solid wastes of the soda ash plant as an adsorbent for the removal of anionic dyes: Equilibrium and kinetic studies, Chem. Eng. J., 138 (2008) 207–214.
[47] G. Alsenani, Studies on adsorption of crystal violet dye from aqueous solution onto calligonum comosum leaf powder, J. Am. Sci., 9(8) (2013) 30–35.
[48] R. Rehman, A. Abbas, S. Murtaza, T. Mahmud, W. Uz-Zaman, M. Salman, U. Shafique, Comparative removal of congo red dye from water by adsorption on *Grewia asiatica* leaves, *Raphanus sativus* peels and activated charcoal, J. Chem. Soc. Pak., 34 (2012) 112–119.
[49] S.B. Hartono, S. Ismadji, Y. Sudaryanto, W. Irawaty, Utilization of teak sawdust from the timber industry as a precursor of activated carbon for the removal of dyes from synthetic effluents, J. Ind. Eng. Chem., 11 (2005) 864–869.
[50] S.S. Bozkurt, Z.B. Molu, Application of corn tassel for the removal of malachite green dye from aqueous solution, Environ. Sci. Pollut. Res., 19(5) (2012) 18–71.
[51] R. Kobiraj, N. Gupta, A.K. Kushwaha, M.C. Chattopadhyaya, Determination of equilibrium, kinetic and thermodynamic parameters for the adsorption of Brilliant Green dye from aqueous solutions onto eggshell powder, Indian J. Chem. Techn., 19 (2012) 26–31.
[52] P.V. Nidheesh, R. Gandhimathi, S.T. Ramesh, T.S.A. Singh, Kinetic analysis of crystal violet adsorption on to bottom ash, Turkish, J. Eng. Env. Sci., 36 (2012) 249–262.
[53] C. Theivarasu, S. Mylsamy, Equilibrium and kinetic adsorption studies of Rhodamine-B from aqueous solutions using cocoa (*Theobroma cacao*) shell as a new adsorbent, Int. J. Eng. Sci. Technol., 2(11) (2010) 6284–6292.
[54] H. Zollinger, "Color Chemistry", VHCA, Wiley-VCH, Zürich, 3rd Edition, 2003, 382.
[55] G. McKay, M. Hadi, M. Taghi Samadi, A. Reza Rahmani, M. Solaimany Aminabad, F. Nazemi, Adsorption of reactive dye from aqueous solutions by compost, Desal. Water Treat., 28 (2011) 164–173.

[56] I.A.W. Tan, A.L. Ahmad, B.H. Hameed, Adsorption of basic dye using activated carbon prepared from oil palm shell: batch and fixed bed studies, Desalination, 225 (2008) 13–28.

[57] S. Izadyar, M. Rahimi, Use of beech wood sawdust for adsorption of textile dyes, Pakistan J. Bio. Sci., 10(2) (2007) 287–293.

[58] V.S. Shrivastava, Removal of Congo red dye from aqueous solution by *Leucaena leucocephala* (Subabul) seed pods, Int. J. ChemTech Res., 4(3) (2012) 1038–1043.

[59] S. Burcă, M. Stanca, C. Indolean, A. Măicăneanu, Industrial waste (sawdust) as biosorbent for dyes removal from waste waters, Acta Tech. Napocensis EESDE, 1(3) (2012) 21–27.

[60] O. Aksakal, H. Ucun, Equilibrium, kinetic and thermodynamic studies of the biosorption of textile dye (Reactive Red 195) onto *Pinus Silvestrys* L, J. Hazard. Mater., 181 (2010) 666–672.

[61] L. Laasri, M.K. Elamrani, O. Cherkaoui, Removal of two cationic dyes from a textile effluent by filtration-adsorption on wood sawdust, Env. Sci. Pollut. Res., 14(4) (2007) 237–240.

[62] L.S. Tan, C.A. Rozaini, Adsorption of textile dye from aqueous solution on pretreated mangrove bark, an agricultural waste: equilibrium and kinetic studies J. Appl. Sci. Environ. Sanitation, 5(3) (2010) 283–294.

[63] P. Janŏs, S. Coskun, V. Pilařová, J. Rejnek, Removal of basic (Methylene Blue) and acid (Egacid Orange) dyes from waters by sorption on chemically treated wood shavings, Biores. Technol., 100 (2009) 1450–1453.

[64] P. Leechart, W. Nakbanpote, P. Thiravetyan, Application of 'waste' wood-shaving bottom ash for adsorption of azo reactive dye, J. Environ. Manage., 90 (2009) 912–920.

[65] M.A.K.M. Hanafiah, W.S.W. Ngah, S.H. Zolkafly, L.C. Teong, Z.A.A. Majid, Acid blue 25 adsorption on base treated shorea dasyphylla sawdust: Kinetic, isotherm, thermodynamic and spectroscopic analysis J. Environ. Sci., 24(2) (2012) 261–268.

[66] R. Rehman, A. Abbas, T. Mahmud, M. Salman, S. Akbar, Thermodynamical and mechanistic studies of Direct Red-28 adsorption on Syzygium cumini stem, J. Chem. Soc. Pak., 34 (5), (2012) 1156–1162 .

[67] D.D. Duong, Adsorption Analysis: Equilibria and Kinetics, Imperial College Press, London, (1998) 49–148.

[68] S.G. Muntean, G.M. Simu, L Kurunczi, Z. Szabadai, Investigation of the aggregation of three disazo direct dyes by UV-Vis Spectroscopy and mathematical analysis, Rev. Chim. Buc. (60)2 (2009) 152–155.

[69] C. Pestişanu, Construcţii, Editura Didactică şi Pedagogică, Bucureşti, 1979.

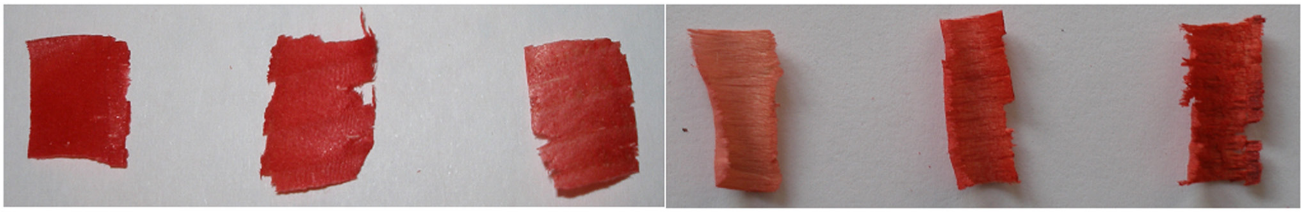

(a) (b)

Fig. S1. Cellulose fiber samples - *Silver Fir* (a), and *Beech* (b) dyed with *DR* dye.

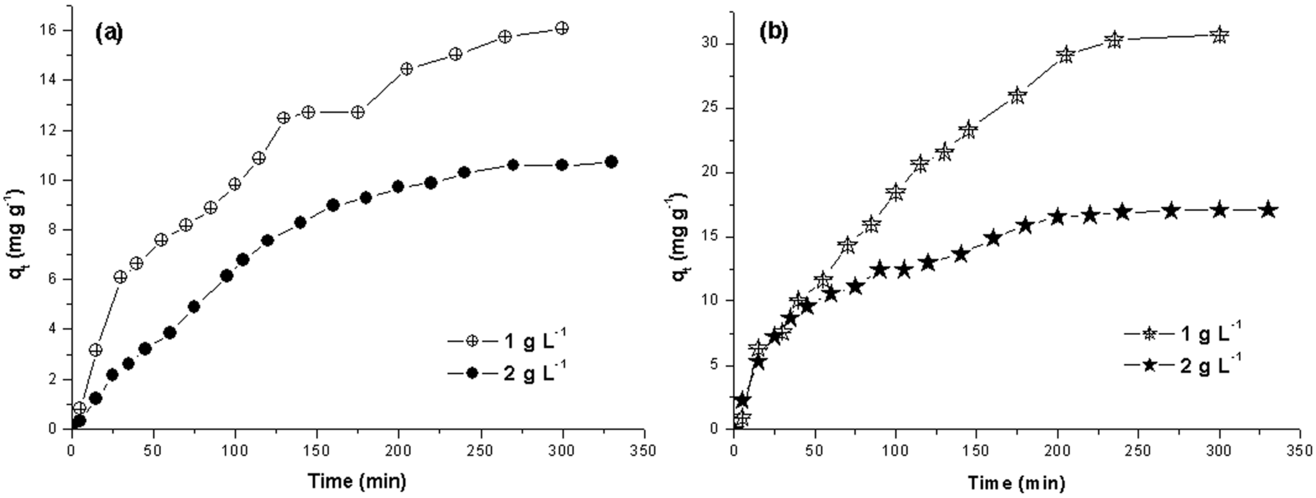

Fig. S2. Effect of fiber dosage. Amount of *DR* dye adsorbed on: (a) *Beech*, (b) *Silver fir* (dye concentration 73 mg L^{-1}, 318 K, pH 6.8).

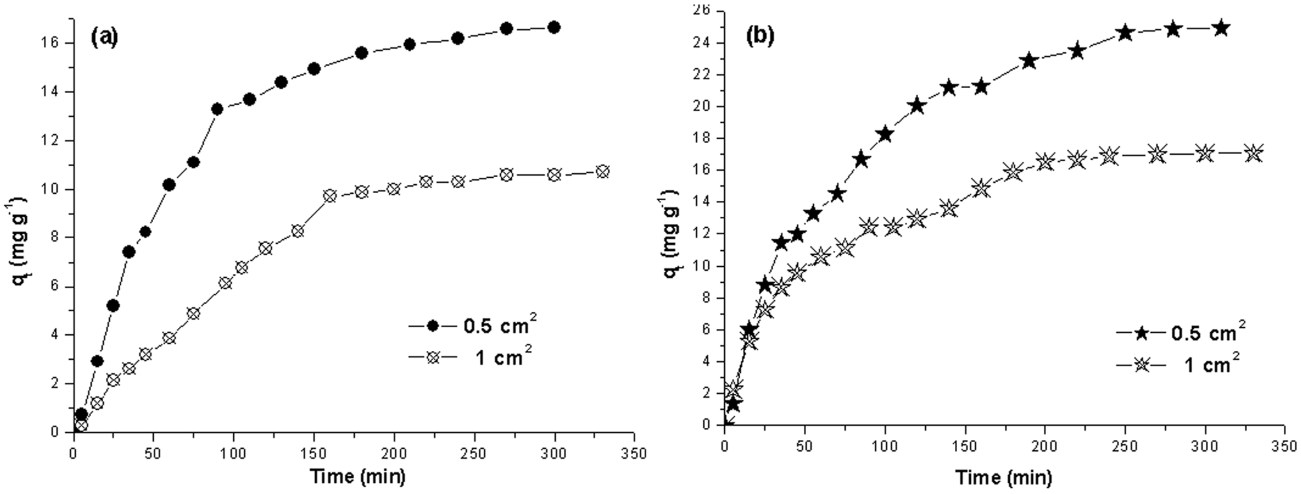

Fig. S3. Effect of fiber specific surface. Amount of *DR* dye adsorbed on: (a) *Beech*, (b) *Silver fir* (pH 6.8 and 318 K, 73 mg L^{-1}, and 0.2 g biosorbent).

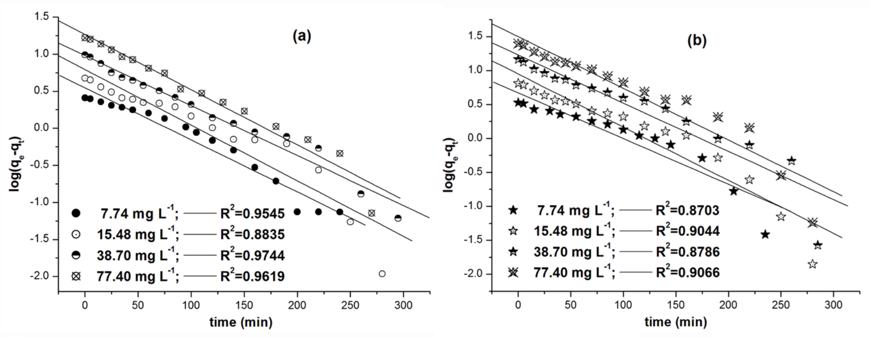

Fig. S4. Lagergren plot for the adsorption of *DR* dye on: (a) *Beech*; (b) *Silver fir* fibre.

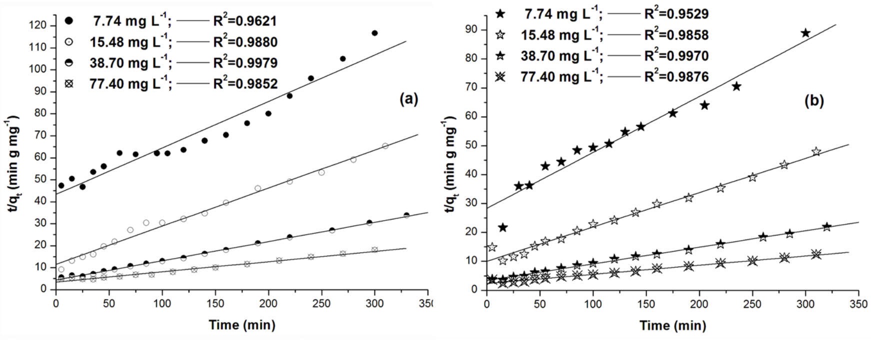

Fig. S5. Pseudo second-order kinetic model fitting for the adsorption of *DR* dye on: (a) *Beech*; (b) *Silver fir*.

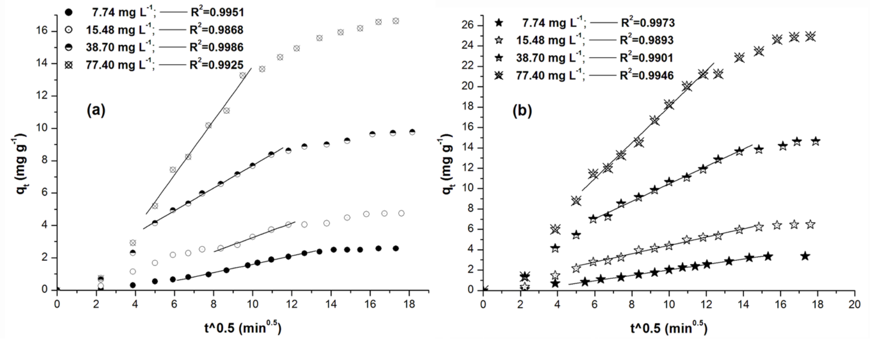

Fig. S6. Intraparticle diffision model fitting for the adsorption of *DR* dye on: (a) *Beech*; (b) *Silver fir*.

Table S1
Comparison of experimental and calculated q_e values and adsorption rate constants for adsorption of *DR* dye on different adsorbents

Sorbent	C_0 (mg L^{-1})	$q_{e,\mathrm{exp}}$ (mg g^{-1})	First order kinetic model		Second order kinetic model		Intraparticle diffusion	
			$q_{e,\mathrm{calc}}$ (mg g^{-1})	$k_1 \cdot 10^3$ (min^{-1})	$q_{e,\mathrm{calc}}$ (mg g^{-1})	$k_2 \cdot 10^4$ (g mg^{-1} min^{-1})	k_i (mg g^{-1} min$^{-0.5}$)	l (mg g^{-1})
Beech	7.74	2.57	3.51	16.20	2.73	25.80	0.26	–0.98
	15.48	4.75	6.21	17.30	5.78	18.25	0.44	–1.19
	38.70	9.77	11.42	15.50	9.58	17.40	0.70	0.71
	77.40	16.63	21.49	17.10	18.39	6.28	1.67	–2.93
Silver Fir	7.74	3.37	4.69	15.50	4.17	13.18	0.27	–0.64
	15.48	6.47	8.89	18.03	8.43	13.99	0.41	0.35
	38.70	14.63	16.99	16.30	16.38	9.79	0.86	1.89
	77.40	24.93	31.57	17.50	28.62	4.21	1.86	–0.61

Table S2
The structural parameters for investigated dye

Parameter/dye	*DR*
Molar mass (g mol^{-1})	737.20
Molecule volume (Å^3)[a]	1782.95
Molecular surface (Å^2)[b]	582.49
Solvent accessible molecular surface (Å^2)[b,d]	1009.43
Volume excluded from contact with solvent (Å^3)[b,d]	502.28
Polar molecular surface (Å^2)[c]	248.15
Principal moments of inertia, I_z (g mol^{-1} · Å^2)[b]	64896.8
Principal moments of inertia, $I_x + I_y$ (g mol^{-1} · Å^2)[b]	65005.29
Ovality[b]	1.91
Globular factor (1/ovality)	0.53
Hydration energy (kJ mol^{-1})[a]	–128.74
ClogP (calculated octanol/water partition coefficient)[b]	7.20
Number of hydrogen-bond donor (pH = 4 ÷ 9)[c]	4.00
Number of hydrogen-bond acceptor (pH = 4 ÷ 9)[c]	13.00

[a] Calculated with the software package HyperChem http://www.hyper.com

[b] Calculated with the software package Chem3D Ultra, http://cambridgesoft.com

[c] Calculated with the software package (online) Marvin, http://www.chemaxon.com./marvin/sketch/index.jsp

Table S3
Parameters of Sips equation

Parameter	*DR*	
	Beech	*Silver fir*
S_{f0} (mg g^{-1})	30.87	33.41
χ	3.83	2.22
K_0 (L mg^{-1})	0.026	0.033
Q/RT_0	1.474	0.972
Q	3345.57	2206.17
n_0	0.37	0.339
β	0.079	0.017
R	0.9962	0.9982